

Autonomous Airborne Wind Energy systems: accomplishments and challenges

Lorenzo Fagiano,¹ Manfred Quack,² Florian Bauer,³ Lode Carnel,⁴ and Espen Oland⁴

¹Dipartimento di Elettronica, Informazione e Bioingegneria, Politecnico di Milano, Italy, 20133; email: lorenzo.fagiano@polimi.it

²Skysails Group GmbH, Hamburg, Germany, 20537; email: m.quack@skysails.de

³kiteKRAFT GmbH, München, Germany, 81737; email: florian.bauer@kitekraft.de

⁴Kitemill AS, Voss, Norway, 5704; emails: lc@kitemill.no, eo@kitemill.no

Xxxx. Xxx. Xxx. Xxx. YYYY. AA:1–30

[https://doi.org/10.1146/\(\(please add article doi\)\)](https://doi.org/10.1146/((please add article doi)))

Copyright © YYYY by Annual Reviews.
All rights reserved

Keywords

airborne wind energy, wind energy, high-altitude wind energy, kite power, energy drones, autonomous aircraft, unmanned aerial vehicle

Abstract

Airborne Wind Energy (AWE) is a fascinating technology to convert wind power into electricity with an autonomous tethered aircraft. Deemed a potentially game-changing solution, AWE is attracting the attention of policy makers and stakeholders with the promise of producing large amounts of cost-competitive electricity with wide applicability worldwide. After pioneering experimental endeavors in the years 2000-2010, since the early 2010s there has been a clear technology convergence trend and steady progress in the field. Today, AWE systems can operate *automatically* with minimal supervision in all operational phases. A first product is also being commercialized. However, all-around *fully autonomous* operation still presents important fundamental challenges, conceptually similar to those of other systems that promise to change our lives, such as fully autonomous passenger cars or service drones. At the same time, autonomous operation is necessary to enable large-scale AWE, thus combining challenging fundamental problems with high potential impact on society and economy. This paper describes the state-of-the-art of the technology with a system perspective and a critical view on some fundamental aspects, presents latest automatic control results by prominent industrial players, and finally points out the most important challenges on the road to fully autonomous Airborne Wind Energy systems.

Contents

| | |
|--|----|
| 1. INTRODUCTION | 2 |
| 2. ANATOMY OF AN AIRBORNE WIND ENERGY SYSTEM | 6 |
| 2.1. On-ground conversion | 7 |
| 2.2. Onboard conversion | 9 |
| 3. FUNDAMENTALS OF AWE REVISITED | 12 |
| 3.1. Tether drag and the scaling dilemma | 12 |
| 3.2. The role of wing loading | 14 |
| 4. ACHIEVEMENTS IN AWE AUTOMATION | 18 |
| 4.1. Automatic on-ground AWE | 19 |
| 4.2. Automatic onboard AWE | 22 |
| 5. AUTONOMOUS AWE: CHALLENGES AHEAD | 24 |
| 6. CONCLUSIONS | 26 |

1. INTRODUCTION

Airborne Wind Energy (AWE) is the technology of harnessing wind power using an autonomous tethered aircraft. This paper considers AWE to convert wind power into electricity. “Airborne” refers to the fact that these systems do not employ a static structure, such as the tower of wind turbines, to constrain the motion of the energy-harvesting element. Rather, the latter exploits the aerodynamic forces to accomplish a prescribed, periodic trajectory in the air, enabled by automatic control. This feature represents one of the main strengths of AWE systems, since it implies low use of energy-intensive materials (concrete and steel) and simple construction, transportation, and installation, ultimately obtaining low capital cost and environmental impact (1). Moreover, the absence of static supporting structures yields another important strength: the possibility to reach high altitudes (about 200-500 m from ground), where the probability distribution of wind is shifted towards high speed values. Since the available power grows with the cube of wind speed, even a rather low increase of the latter can dramatically augment the energy yield of a given system. These advantages are counterbalanced by a rather high system complexity, where automation plays a central role. To be a valid addition to the existing portfolio of renewable energy technologies, it is imperative that AWE systems demonstrate highly reliable, automated operation over prolonged time periods at reasonable cost. Such a high reliability level is currently one of the main standing challenges, as argued later on.

The term AWE has been coined around the year 2010, when several stakeholders, mainly companies but also academic research groups, agreed on a common term for the different concepts being researched, all sharing the mentioned characteristic trait. Indeed, from the roots planted by theoretical works published in the late 1970s (2, 3), several real-world systems have been developed since the early 2000s, initially under names such as kite power, energy kites, or high-altitude wind power/energy. The various developments differentiated in terms of aircraft type (flexible, semi-rigid, rigid), number of tethers (one to three), lift type (aerodynamic or aerostatic), and position of the electric machines and power converters (onboard or on the ground). While the decade 2000-2010 (and particularly the second half of that decade) has seen a growing number of research and development endeavors with different concepts, since the early 2010s there has been a clear technology convergence

trend, as more and more knowledge was being gathered. Today, all of the systems that appear to be close to industrialization employ the so-called crosswind motion (see the sidebar “fundamentals of AWE systems”), and almost all of them feature a single tether. Two

FUNDAMENTALS OF AWE SYSTEMS

Crosswind motion

This term refers to a flown path that extends mainly on a surface roughly perpendicular to the wind flow. Thanks to the constraint imposed by the tether, the aircraft speed in crosswind motion is much larger than the wind speed, of a factor roughly equal to the total glide ratio (i.e., lift-to-drag ratio) of the wing and tether. This results in large aerodynamic forces that can both sustain the aircraft and yield significant mechanical power values. Also the blades of conventional wind turbine exploit crosswind motion, however in this case their trajectory is stabilized by the rotor and tower, while in AWE it is realized by active control.

On-ground power conversion

In this energy conversion strategy, also known in the literature as “pumping power”, the system repeatedly carries out a traction phase and a retraction one. In the former, the tether is reeled-out from a drum installed on the ground, under large pulling force obtained during crosswind motion. In the retraction, the aircraft is steered on a path with low aerodynamic forces, and the tether is reeled-in at low power cost. The employed tether is made of polymeric materials and transfers mechanical power only.

Onboard power conversion

In this approach, also referred to as “drag power”, the rigid aircraft features relatively small turbines, together with the required power converters. Thanks to the speed augmentation effect of crosswind motion, these turbines generate rather large electric power which is transferred to ground via the tether, at a voltage level that depends on the system size (for example the Makani M600 prototype featured 4kV transmission over the tether). The tether, comprising both a load-bearing part and a power-conducting one, is reeled-out only to take-off and reach the operational altitude, then it is kept at constant length during power generation.

power conversion principles are being pursued, depending on where the electric machine(s) and power electronics are installed: either on-ground (pumping power conversion) or onboard. For on-ground conversion, either a flexible or a rigid wing is used, while onboard conversion is feasible only with a rigid aircraft, resulting in total in three system layouts that are currently the most promising ones, represented in Figure 1. Each layout has distinct advantages and disadvantages, and there is a general consensus in the AWE R&D community that, at the current stage, all three shall be further investigated and may eventually be viable in different market segments. For example, on-ground systems with flexible wings generally feature lower wing loading, allowing them to start operating in lighter wind, while those based on rigid wings with onboard propellers have better control authority outside the nominal design conditions and can carry out faster retraction phases. Systems with onboard generation can avoid the presence of phases with power consumption (depending on the wind speed) but generally require higher wind speed to operate, due to the larger

wing loading and tether mass. Take off and landing strategies and energy management for the onboard sensors and actuators are other aspects where these three concepts differ significantly.

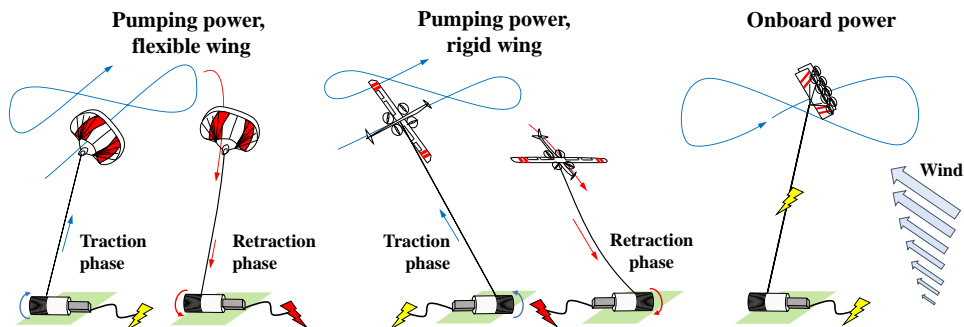


Figure 1

Operation principle of the three AWE system layouts that are currently in advanced development stage. From left to right: on-ground flexible, on-ground rigid, and onboard power conversion.

Deemed a potentially game-changing solution (4), AWE is attracting the attention of policy makers and stakeholders, like the European Commission (5) and many national governments, with the promise of producing large amounts of cost-competitive electricity with wide applicability worldwide. For example, it is estimated that, in the EU, 100% of electricity demand could be supplied by AWES exploiting 1% of land (5), not to mention the huge potential of offshore sites. Such an interest is the result of the continued efforts of entrepreneurs and researchers over the last 20 years. AWE is in fact an inspiring, multidisciplinary renewable energy technology enabled by automatic control, receiving ever-increasing attention from researchers motivated by the related challenges. These include control and optimization aspects, see e.g. (6, 7, 8, 9, 10, 11, 12, 13, 14, 15, 16, 17, 18, 19, 20, 21, 22), modeling and identification (23, 24, 25, 26), estimation (27, 28), design (29, 30), aerodynamics and theoretical limits (31, 32), system design and testing and performance assessment (33, 34, 35, 36, 37), power conversion (38), energy yield and economic aspects (39, 40, 41), safety and reliability (42, 43, 44), and resource assessment (45, 46, 47). Several surveys and tutorial papers on AWE appeared in the last decade (48, 49, 50, 51), as well as two edited books (52, 53). The Airborne Wind Energy Conference series has reached now the 9th edition and is held bi-annually since 2013, and the European association Airborne Wind Europe has been founded in 2019, with the goal to promote the development of this technology particularly towards aspects such as public engagement and support, regulations (e.g., concerned with the airspace), and standards. Moreover, several companies, like Skysails Power (DE, <https://skysails-power.com/>), Kitemill AS (NO, <https://www.kitemill.com/>), kiteKRAFT GmbH (DE, <https://www.kitekraft.de/>), Kitepower BV (NL, <https://thekitepower.com/>), Kitenergy Srl (IT, <http://www.kitenergy.net/>), Skypull SA (CH, <https://www.skypull.technology/>), Windlift (USA, <http://www.windlift.com/>), Enerkite GmbH (DE, <http://www.enerkite.com/>), TwingTec AG (CH, <http://www.twingtec.com/>), Ampyx Power BV (NL, <http://www.ampyxpower.com/>), are developing these systems towards commercialization, with a steady average progress of the sector amid notable ups and downs. In 2020, the company Makani ceased operation due to insufficient

funding, after an engaging decade-long thrust to upscale their technology and demonstrate a 600-kW system offshore (54). The analysis of the large amount of documents and data that the company generously made public (55) reveals that rather few hours of supervised automatic operation were carried out. Fully autonomous operation, albeit necessary for the technology to eventually become commercial at large scale, was not yet considered at the current development stage. In 2021, the company Skysails Power announced the production of their first pre-series with 80kW cycle power (56). The system operates automatically in all phases under minimal supervision.

Overall, there is good progress in *automatic* system functioning in the various operational phases, however the road to all-round *fully autonomous* and largely unattended operation appears to be still difficult: it presents fundamental challenges conceptually similar to those of other autonomous systems that promise to change our lives, such as fully autonomous passenger cars or service drones. Fully autonomous operation is clearly necessary for the development and commercialization of AWE in farms of tens or hundreds of MW-scale units (see Figure 2), as envisioned in the decade 2030-2040 and required to significantly contribute to meet the global sustainability and climate change mitigation targets. Thus,



Figure 2

Concept rendering of large-scale deployment of AWE systems. Most technology developers envision single units in the MW-range, arranged in wind farms. Image courtesy of the SkySails Group.

the mentioned challenges are at the same time fundamentally difficult and practically crucial, motivating a continued support to research and development efforts. A risk-controlled, target-driven approach centered on public support and public-private collaboration is indeed proposed in a recent study (5) as the main way to develop the AWE sector.

In the described context, the main goal of this review paper is to summarize the accomplished results in AWE automation (Section 4), referring in particular to the three most promising layouts mentioned above, and to describe the main standing challenges to obtain fully autonomous systems (Section 5). To properly contextualize these contributions, a more detailed description of the layouts and their operation will be given (Section

2), as well as an analysis of crucial and often overlooked theoretical aspects (Section 3). The material presented in the remainder includes contributions provided by three prominent companies that are representatives of the considered concepts, thus providing also an industrial viewpoint on autonomous AWE.

2. ANATOMY OF AN AIRBORNE WIND ENERGY SYSTEM

An effective way to analyze an AWE generator is to derive its functional diagram, i.e. a block diagram that, starting from the principal function of the whole system, presents in a tree-like structure the various required sub-functions. This kind of analysis is typical of engineering design and it can reach a deep level of detail. The functional diagram shown in Figure 3 applies to all AWE concepts considered in this review. Note that a large number

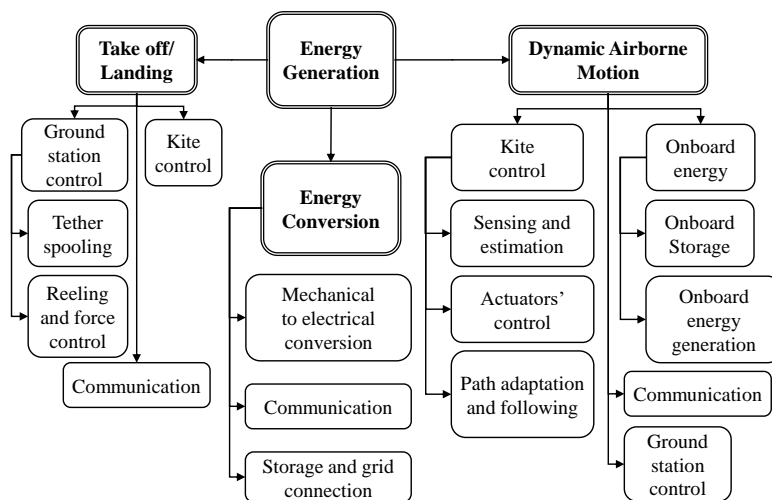


Figure 3

Example of functional diagram of an AWE system. It is limited at a rather high level in the interest of space: for example, the kite control function required to achieve take-off/landing implies a number of additional sub-functionalities, like those shown in the dynamic airborne motion branch. In a complete diagram, the analysis is deepened to elementary functions. Some sub-functions appear more than once in the diagram, as they pertain to different parent functions: for example, suitable ground-station control functionalities must be present to accomplish both take-off/landing and dynamic airborne motion of the aircraft, with different requirements.

of the presented functions require feedback control, in addition to solutions pertaining to mechanics, electric systems, sensors, materials, and aerodynamics. The functional diagram provides a good idea of the tasks to be accomplished and of the complexity arising from the interaction among the aircraft, the tether, and the ground station.

Starting from the functional diagram, a suitable system layout is selected and the various subsystems and components are designed in order to achieve the wanted functionalities. As a result, a system architecture is obtained, like the one presented in Figure 4, that contains the main subsystems together with the functionalities they accomplish. The next sections describe, for the three considered AWE concepts, specific solutions that are representative of the state-of-the-art in AWE. They differ substantially in terms of mechanical

and electrical layout and control aspects, while they have rather similar sensor setups. In particular, all AWE systems employ an Inertial Measurement Unit (IMU) comprising three-axial accelerometers, gyroscopes, and magnetometers, global positioning devices, load cells to measure the tether force, and possibly airspeed sensors. Tether length, angle, and speed are measured as well on ground, as well as ground wind speed and direction. More details on filtering and estimation of AWE systems can be found in (27, 57, 28). As apparent from Figure 4, AWE is a highly multidisciplinary technology involving mechanics, aeronautics, control, electrical engineering, and materials. In the interest of space, several notions of these aspects are given for granted in the remainder; the interested reader can find more details in AWE-specific literature, most notably the edited books (52, 53).

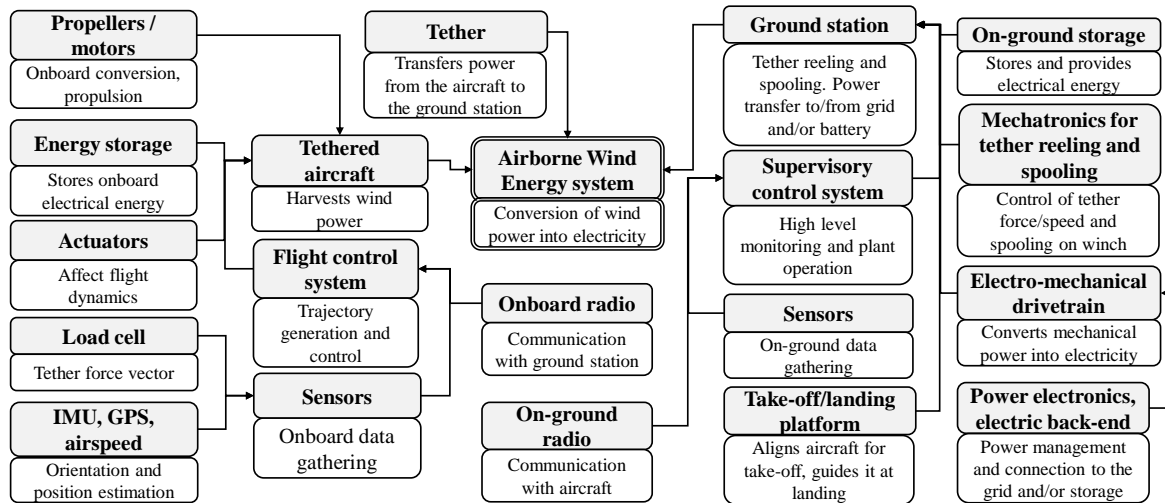


Figure 4

Example of AWE system architecture with the main subsystems and the functions they accomplish.

2.1. On-ground conversion

As shown in Figure 1, in pumping conversion systems the electric machine and power converters are installed on the ground. The main tether is made of braided ultra-high molecular weight polyethylene (UHMWPE) fibers, with a breaking load 8-10 times higher than steel of the same mass. The density of this material is about 980 kg/m^3 , just below that of water. Figure 5 presents the breaking load of a commercial UHMWPE rope as a function of its diameter. As an example, a 200-m-long, 3-mm-diameter tether has a minimum breaking load of about 10000 N and its mass is about 1.4 kg. However, this material is subject to creep, which shall be properly taken into account (30). It is also sensitive to heat, with a melting point of about 150°C , which imposes particular care to limit tether friction in the ground station. The latter includes a winch connected to the electric motor/generator via a gearbox, an active tether spooling system, various sensors (tether force and angles, wind speed), and the power electronics to connect to the grid and/or a battery storage system. The system features the following main operational phases: take-off, transition to power generation, pumping operation, transition to landing, and landing.

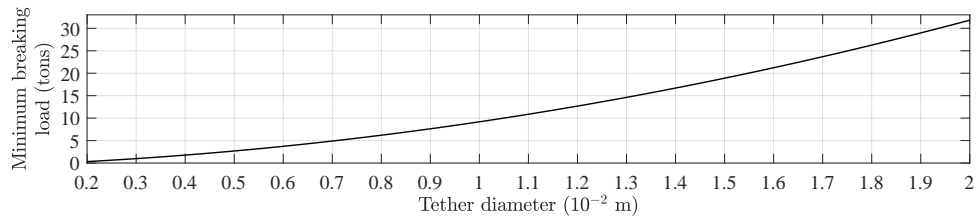


Figure 5

Minimum breaking load of a commercial UHMWPE rope as a function of its diameter.

The pumping operation phase features four sub-phases: traction, transition to retraction, retraction, and transition to traction. The main differences between systems that employ a flexible wing and those with a rigid one are in the take-off/landing strategy, retraction trajectory, and onboard actuation, as further detailed in the next sub-sections.

2.1.1. Flexible-wing systems. To describe the main features of on-ground AWE with flexible wings, we refer to the Skysails Power SKS PN-14 system, shown in Figure 6, which is being produced and commercialized in a pre-series at the time this paper is being written (56). It



Figure 6

Left: Skysails Power SKS PN-14 system, with ① ram-air kite, ② control pod with steering mechanism (see (58)) ③ main tether, ④ launch- and landing mast, ⑤ 30ft container housing the ground station, ⑥ winch with generator and gearbox, and ⑦ flat rack with ring mount on concrete foundation plate. Right: the SKS PN-14 in operation. Courtesy of the SkySails Group.

employs a ram-air kite (leading-edge-inflated ones, or LEI, are used by other flexible-wing AWE developers, such as Kitepower BV) with a control pod hosting the onboard sensors, actuators, flight control system and onboard energy storage/generation system. The ground station is installed on a rotating platform to adjust to the wind direction, and it features a launch and landing mast. The kite takes off when the lift is large enough to keep it airborne and obtain a positive average power in the pumping cycle. In the case of the SKS PN-14, the system can be launched starting from 3-m/s average wind speed. A secondary, thinner tether attached to the leading edge is used to guide the kite from/to the mast for the launch and landing operations. The mast has to be tall enough to leave enough space for the kite to fully deploy and maneuver in safe conditions. After detaching from the mast, the kite lifts in the air while both tethers (the main and the secondary ones) are reeled-out until reaching an altitude suitable to transition to power generation. In the traction phases, the kite follows figure-eight patterns, while in the retraction phase it transitions to the border of the so-called power zone, where an almost-stationary azimuth-elevation position is kept while the tethers are reeled-in to start a new pumping cycle. The landing procedure is the reverse of the launching one: the kite is flown to the border of the power zone and then pulled to the mast, first by the main tether and then by the secondary one. Specifically, the SKS PN-14 has a 800-m-long main tether, allowing it to operate between 200 and 400 m above ground. It achieves an average cycle power higher than 80 kW, depending on the site. The ground station is designed as a 30-ft container, which facilitates transport even to remote locations.

2.1.2. Rigid-wing systems. We consider the 7.4-m-wingspan Kitemill KM1 prototype (Figure 7) to describe the main features of on-ground, rigid-wing AWE systems. The aircraft features a slender design with high glide ratio, similar to a sailplane, allowing it to reach large crosswind speed values. Onboard vertical-axis propellers are used for the take-off and landing phases (vertical take-off and landing - VTOL), which are carried out in hovering mode, like a multi-copter drone. This makes it possible to use a platform very close to ground and to avoid using a secondary tether, at the cost of a higher onboard mass and complexity of the aircraft. The propellers on the wings can be tilted to face the apparent wind during operation and used as turbines to generate energy for the onboard systems. During dynamic airborne motion, the trajectory is governed by acting on discrete control surfaces (ailerons, elevator, rudder). Besides the aircraft structure and the take-off and landing phases, the other main difference with respect to flexible-wing systems is the retraction phase, which in rigid-wing systems can be carried out by gliding upwind, (22). The KM1 features an average output of 20 kW and its goal is to develop and test the system functionalities towards fully autonomous and reliable operation, before scaling up.

2.2. Onboard conversion

The main operational phases of AWE systems with onboard conversion are the same five listed for on-ground ones. However, thanks to the use of onboard turbines and electric machines, the power generation phase is simpler, as it consists of a single operation mode where the aircraft flies a periodic pattern at constant tether length. The power output changes periodically along the pattern, and in principle this concept can operate without periods of power consumption, depending on the system design and wind conditions. The closest representation to a full-scale AWE system with onboard generation is currently the



Figure 7

Kitemill KM1 prototype. Clockwise from left: aircraft with onboard propellers, omnidirectional launch and landing platform, on-ground winch connected to the electric machine.

Makani M600, see Figure 8 and (54, 55). It features a ground station with a winch to

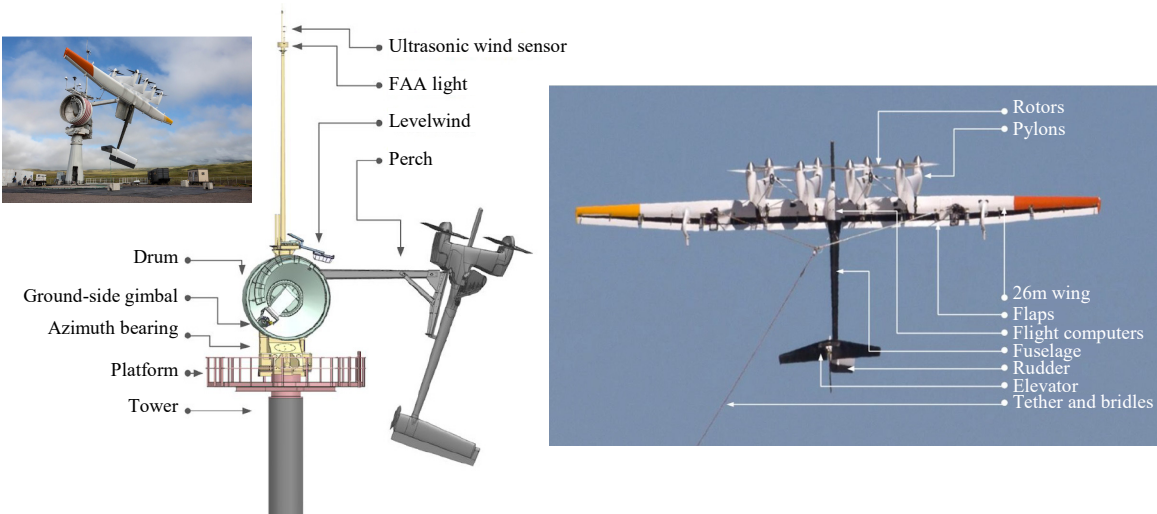


Figure 8

Main components of the Makani M600 ground station and aircraft. Figures adapted from (55).

store the tether and a perch/landing platform. The aircraft has eight onboard turbines linked to electric generators, which act respectively as propellers and motors during VTOL (and during dynamic flight if needed). The development strategy adopted by Makani has been to quickly scale up their system to a size close to commercial medium/large-scale wind turbines. According to (55), this decision made it difficult or impossible to correct substantial design mistakes, which in turn led to poor power conversion performance. As an example, the system had very poor roll control authority during hovering, making it highly susceptible to wind disturbance, and also small roll capability because of the designed bridle, making it hard to generate centripetal forces during turns in aircraft mode and hence to obtain the desired flight paths. The cumulative number of test hours reported in (55) with the M600-series is less than 30 over a period of more than 2 years. The Makani experience had anyway the merit to attract attention on AWE technologies and to show that these devices can be up-scaled and deployed offshore, a phase that most companies are eventually targeting after accumulating a much larger base of experience and flight hours and higher reliability at lower scale. Moreover, the documents and data made accessible by Makani contains useful information regarding large-scale design, testing and operation of onboard AWE.



Figure 9

kiteKRAFT functional prototype. Clockwise from left: landed, aircraft mode, hovering mode.

The German company kiteKRAFT GmbH is developing an onboard AWE system, currently being tested at small scale, introducing solutions that overcome the drawbacks of the M600 design (59). The aircraft (see Figure 9) has a boxplane planform with high-lift multi-element airfoil and with H-empennage. The rotors are mounted in front of the wings close to their tips. The boxplane yields high strength and stiffness at low mass and

with low induced drag. The H-empennage offers the possibility for tailsitter launching and landing if needed, and passive and active stability means of angle of attack and angle of sideslip during crosswind flight, as well as passive pitch stability during hovering with the 90° rotatable elevator. The main wings’ flaperons are in the rotor downwash, offering roll control authority during hover, differently from the Makani prototype. Each rotor has fixed pitch, optimized for high efficiency propeller- and wind turbine-mode¹, and is connected to a brushless DC motor/generator with direct drive and AC/DC power electronics operated in field oriented current control and superimposed moment- and speed control. The kite and ground station have redundant control units, communication buses, and sensors to enable fully autonomous and robust operation. The bi-directional power is transmitted over 800 V DC² electric cables: several small insulated ones are used to obtain a small tether diameter and a high level of fault tolerance (60). In the tether, the electric cables together with communication ones are wound helically around a Kevlar core, which takes the mechanical load while being light-weight and heat resistant. The ground station converts the tether voltage to AC grid voltage, has a winch to store the tether when the kite lands, and has a perch/landing platform for the kite. The kite flies figures of eight, avoiding the need for slip-rings and tether “de-twisting” devices (55).

3. FUNDAMENTALS OF AWE REVISITED

The equations of crosswind kite power published by M. Loyd (3) are arguably those that laid the first theoretical foundations of Airborne Wind Energy science, and also ignited the spark for many pioneering experimental developments in the 2000s. Many subsequent studies started from those equations to estimate the energy yield, scalability and economics of AWE systems, and also investigated further aspects by adding more details to the first version, leading to so-called quasi-steady models, see e.g. (61). A recent overview of the theoretical derivation is provided in (51). As a matter of fact, the very first equations in (3) cannot be applied directly for power estimation, as among others the following three main aspects are neglected: a) losses due to the angular displacement between the tether and the prevalent wind (so-called cosine-cube losses, see e.g. (62, 55, 51)); b) tether drag (63, 7, 8, 64); c) aircraft mass per unit area, which we refer to as (minimum) wing loading, w_l (61, 62). In this review paper we elaborate on the latter two aspects, since their implications are apparently not fully examined in the literature, while on the other hand cosine-cube losses are well understood. As a first approximation, these additional aspects can be still analyzed with rather simple equations derived from a force equilibrium, similarly to the original Loyd’s equations.

3.1. Tether drag and the scaling dilemma

Starting with tether drag, its inclusion makes it possible to appreciate an often overlooked aspect in AWE development: high altitude winds are most efficiently harvested by large scale systems. Before presenting the equations that justify this statement, we comment on its consequences: development and testing at small-scale, which is more convenient in terms

¹The rotor area is chosen large enough to obtain a low disc loading in both modes and thus high efficiency as well as moderate induced speeds over the wings.

²The voltage depends on the system size. Up to 100 kW nominal power, 800 V is used, above that power, 1 to 4 kV is used.

of time and cost, can be done by operating only at relatively low altitude from ground, where the full potential and advantages of AWE systems are not realized. On the other hand, to properly harness high-altitude wind (e.g., above 300 m from ground) one requires a large-scale system, with higher development time, cost, and risk. This leads to a *scaling dilemma*: shall one first improve the Technology Performance Level (TPL) at low scale, knowing that this won't lead to a marketable product nor to a system able to optimally extract high-altitude wind, and then upscale the system to improve the Technology Readiness Level (TRL) up to entering the market, or shall one try to upscale sooner (higher TRL) to reach a marketable size, and then improve and optimize the TPL at large scale?

The choices made by the various AWE developers in the past decade show that the answer is not trivial, as it is affected by many factors. In a world where investments in startups and high-tech companies are expected to yield a positive return in two to five years, and where renewable power generation technologies such as wind and solar have reached maturity and are thus very difficult to compete with in the market, companies that relied mainly on venture capital and could not secure continued funding have been pushed on the second path, i.e., upscale as soon as possible. For AWE systems, this turns out to be too risky, as the story of Makani has taught to the whole sector. Indeed, all developers are currently pursuing an approach, based on gradually increasing investments, to improve the TPL at low scale, demonstrating more and more functionalities until reaching high reliability and continuous operation, and eventually increasing the TRL through up-scaling. This path has clearly a better profile in terms of investment risk, but for the technology at hand requires continued private and, most importantly, public support (5), as it happened (and is still happening) for more mature renewable technologies.

To see where the scaling dilemma stems from, let us consider a system with on-ground conversion (similar considerations hold for onboard conversion). Figure 10 presents a sketch of the considered model and the notation. The traction force acting on the tether, assuming an optimal reel-out speed of $\frac{1}{3} W \cos(\theta)$ and including the drag contributed by the tether itself, reads (63, 7, 8):

$$F = \frac{2}{9} \rho A C_L E(F, c_s)^2 \left(1 + \frac{1}{E(F, c_s)^2}\right)^{\frac{3}{2}} (W \cos(\theta))^2, \quad 1.$$

where ρ is the air density, and

$$E(F, c_s) = \frac{C_L}{C_D + \frac{C_{D,t} l_t d_t(F, c_s)}{4A}} \quad 2.$$

is the total glide ratio, considering both the aircraft (whose un-tethered glide ratio is $G = C_L/C_D$) and the tether. In equation 2., c_s is the design factor considered when dimensioning the tether (for example, a value $c_s = 3$ is suggested in (30) for a tether lifetime ≤ 2 years), and $d_t(F, c_s)$ indicates that the tether diameter is automatically sized in order to have a minimum breaking load (see Figure 5) equal to the traction force F multiplied by the prescribed design factor. Equations 1. and 2. can be easily solved numerically. Then, the cycle power can be estimated as:

$$P = \eta F \frac{W \cos(\theta)}{3} = \eta \frac{2}{27} \rho A C_L E(F, c_s)^2 \left(1 + \frac{1}{E(F, c_s)^2}\right)^{\frac{3}{2}} (W \cos(\theta))^3. \quad 3.$$

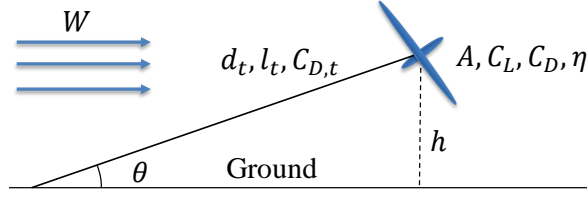


Figure 10

Model used to evaluate the effect of tether drag as a first approximation. W is the wind speed magnitude, $d_t, l_t, C_{D,t}$ the tether diameter, length, and drag coefficient, A, C_L, C_D the aircraft's lifting surface, lift coefficient, and drag coefficients (assuming operation at the nominal angle of attack), η is the pumping cycle efficiency, h is the aircraft's altitude from ground.

On the other hand, by neglecting the tether drag we have (3, 8):

$$\bar{P} = \eta \frac{2}{27} \rho A C_L G^2 \left(1 + \frac{1}{G^2}\right)^{\frac{3}{2}} (W \cos(\theta))^3. \quad 4.$$

It is clear that equations 3. and 4. differ only by the glide ratio, which in the first case is affected by the tether, suitably sized to withstand the generated load. Figure 11 presents the ratio P/\bar{P} and the values of P and $E(F, c_s)$ for an hypothetical soft kite (larger A and lower G) and a rigid aircraft (smaller A and higher G), with various A values and increasing altitude from ground h , which, with fixed elevation θ , correspond to increasing tether length l_t (thus increasing tether drag), also shown in Figure 11. It can be noted that: 1) the tether has a leveling effect on the total glide ratio: for aircrafts with higher G there is a steeper decrease and then a plateau towards lower glide ratios, while aircrafts with lower G experience a moderate decrease, since their speed is already lower and the effect of tether drag is relatively less impacting; 2) for the same operating altitude, the gap between P and \bar{P} improves with larger lifting surface, i.e. at larger scale, as anticipated. Note that the fact that larger A values help to mitigate the effect of tether drag on the total glide ratio has been already pointed out in the literature, see e.g. (8), however without considering a proper tether re-dimensioning as A increases, which reduces the extent of the advantage gained with larger size. Finally, note that in Figure 11 lower altitude values are not feasible for larger systems, due to limitations on the minimum turning radius as a function of the aircraft wingspan (i.e., larger systems are not able to operate with too short tethers, an aspect not treated here). The obtained numerical values are specific to the considered parameters (for example, several AWE developers using rigid aircrafts declare C_L higher than 2) and may vary depending on the specific operational factors, such as the reeling strategy, however the general trends remain, as they are intrinsic in how the tether drag affects the aircraft's total glide ratio.

3.2. The role of wing loading

Regarding the effect of the aircraft's mass per unit area (minimum wing loading, w_l), rather detailed analyses are reported in (61) for traction power, where the effect of kite mass is studied considering either power conversion or propulsion of a ground or marine vehicle, and in (62) for take-off of rigid-wing systems. Both studies indicate the importance of the airborne mass, which had been neglected for simplicity in (3) under the assumption that the

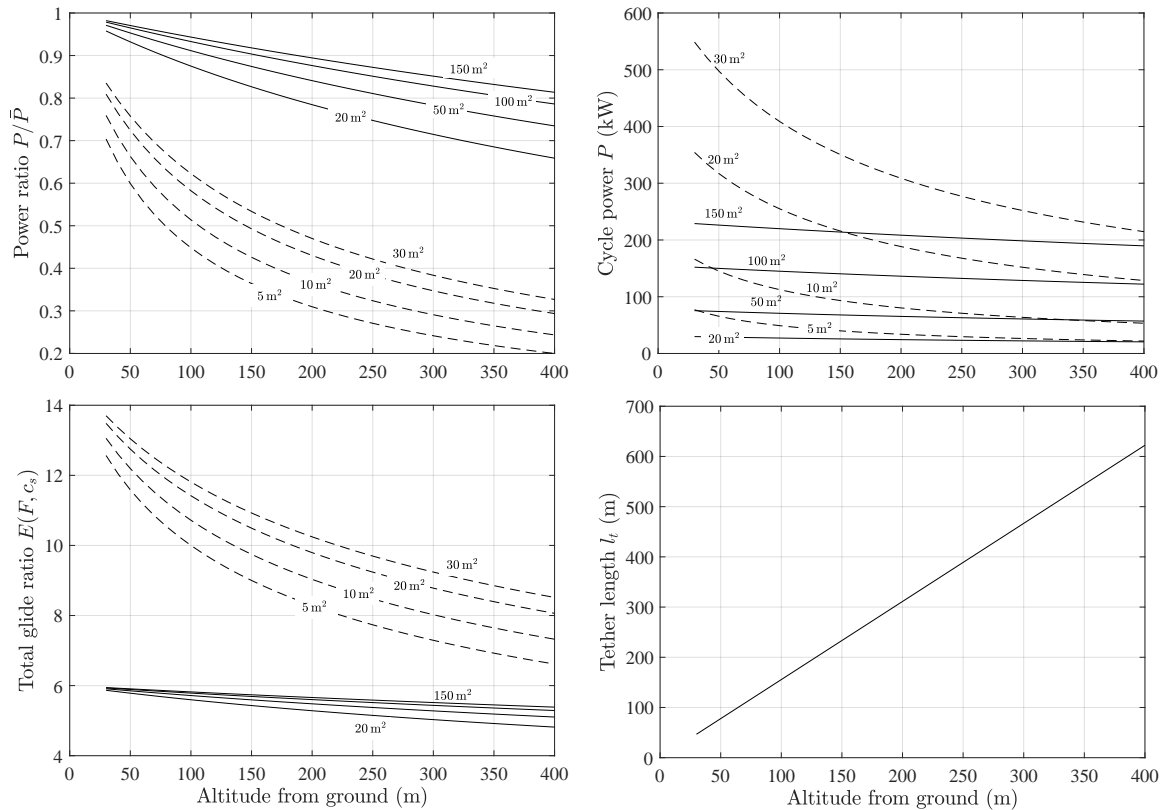


Figure 11

Effects of tether drag on system performance for on-ground AWE systems, with uniform wind speed $W = 12$ m/s, $\theta = 40^\circ$, $\rho = 1.2$ kg/m³, tether drag coefficient $C_{D,t} = 1$. Clockwise from top left: power ratio P/\bar{P} , cycle power P (kW), total glide ratio $E(F, c_s)$, tether length l_t (m). Solid lines: soft wings (lift coefficient $C_L = 1.2$, glide ratio $G = 6$, cycle efficiency $\eta = 0.5$) with lifting surface $A = 20, 50, 100, 150$ m². Dashed lines: rigid wings (lift coefficient $C_L = 2$, glide ratio $G = 15$, cycle efficiency $\eta = 0.7$) with lifting surface $A = 5, 10, 20, 30$ m².

lift force \vec{F}_L generated by the aircraft is much larger than its weight, \vec{F}_w . This assumption is often still considered to be valid in the AWE community, however it becomes highly inaccurate if we consider the projection of \vec{F}_L on the direction of \vec{F}_w and flight directions pointing upwards, which is what matters to keep the aircraft airborne.

In other words, without considering the aircraft mass one may compute flight trajectories that yield a large traction power, but that as a matter of fact could never be flown by the aircraft because it's too heavy, thus requiring an injection of power either in the form of reel-in speed (for on-ground systems) or propellers' thrust (for onboard systems), ultimately reducing the power performance or even leading to an overall negative power balance.

We highlight here the link between w_l and the minimum wind speed at which the system can start to fruitfully operate, the so-called cut-in wind speed. Again, we consider an on-ground system and we rely on a rather simple model, presented in Figure 12, where the aircraft is assumed to be in a given position (θ, ϕ, l_t) , with given reel-out speed \dot{r} and velocity angle γ .

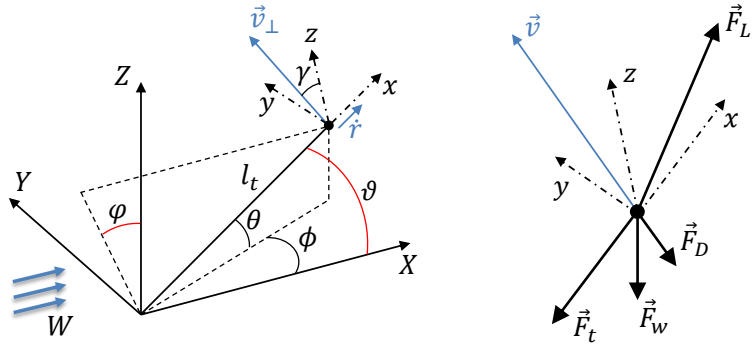


Figure 12

Model used to evaluate the effect of wing loading on the minimum wind speed required to operate. (X, Y, Z) and (x, y, z) are the inertial and local (tether) reference systems, respectively. \vec{v} is the apparent velocity vector, i.e., the vector sum of the absolute wind minus the kite velocity relative to ground. \vec{v}_\perp and \dot{r} are the projections of the kite velocity relative to ground onto the (y, z) -plane and the x direction, respectively, γ is the “velocity angle” (i.e., the angle between vector v_\perp and the z direction) or flight direction (9, 17). θ, ϕ are the elevation and azimuth angles, ϑ, φ the wind window angles (see (17)), finally $\vec{F}_L, \vec{F}_D, \vec{F}_t, \vec{F}_w$ the lift, drag, tether pull, and weight force vectors. It is assumed that the tether is straight, so that its length l_t corresponds to the distance of the kite from the origin of (X, Y, Z) . Note that different sources may adopt different conventions for the coordinate systems, for example in (17) the Z axis points down and the Y axis completes a right-handed system accordingly.

We set as variables to be determined the three-dimensional (3D) lift force vector \vec{F}_L , the tether force \vec{F}_t (assumed to be pointing to the origin, so that only its magnitude $|\vec{F}_t|$ needs to be determined), the wind speed magnitude W (assuming that the wind vector is aligned along the X -axis, see Figure 12), and the magnitude of \vec{v}_\perp (whose direction is determined by the imposed velocity angle γ). For physical consistency, these six variables shall satisfy the following set of five nonlinear equations:

$$\vec{F}_L + \vec{F}_D + \vec{F}_t + \vec{F}_w = 0 \quad 5a.$$

$$|\vec{F}_L| = \frac{1}{2} \rho A C_L |\vec{v}|^2 \quad 5b.$$

$$\vec{F}_L \cdot \vec{v} = 0 \quad 5c.$$

Namely, the vector equation 5a. imposes the 3D equilibrium among the involved forces, while 5b. and 5c. impose that the lift force vector has a magnitude consistent with the aerodynamics and is perpendicular to the apparent wind vector, respectively (\cdot denotes the inner product). Analyzing the manifold of points satisfying equation 5. for a given prescribed flight condition (or even for a whole discretized path, see e.g. (61)) can give useful insight on the wind speed/traction force combinations that are feasible in such a condition (quasi-steady model). In particular, minimizing W subject to 5. yields the minimum wind speed such that said flight condition is feasible. To estimate the cut-in wind speed we analyze here a single position downwind $(\theta, \phi, l_t) = (35^\circ, 0^\circ, 100)$, choose $\dot{r} = 0$ (zero reeling velocity, so that no mechanical power is neither injected, nor generated at ground), consider velocity

angles ranging from $\gamma = 0^\circ$ (aircraft pointing up) to $\gamma = 90^\circ$ (level flight), and solve:

$$\underline{W} = \min_{\vec{F}_L, |\vec{F}_t|, W, |\vec{v}_\perp|} W, \text{ subject to equations 5.} \quad 6.$$

For the purpose of illustration, we set $A = 20 \text{ m}^2$, $C_L = 1.2$, $G = 15$, and solve 6. with increasing values of wing loading w_l . Regarding the tether, we set $d_t = 0.015 \text{ m}$ and also include part of its mass in the total airborne mass (61). In the considered condition, with $\gamma = 0$ the setup is very similar to the winch launch analyzed in (62), however now the unknown is the wind speed instead of the reel-in speed required for take-off. Figure 13 (left) presents the obtained results.

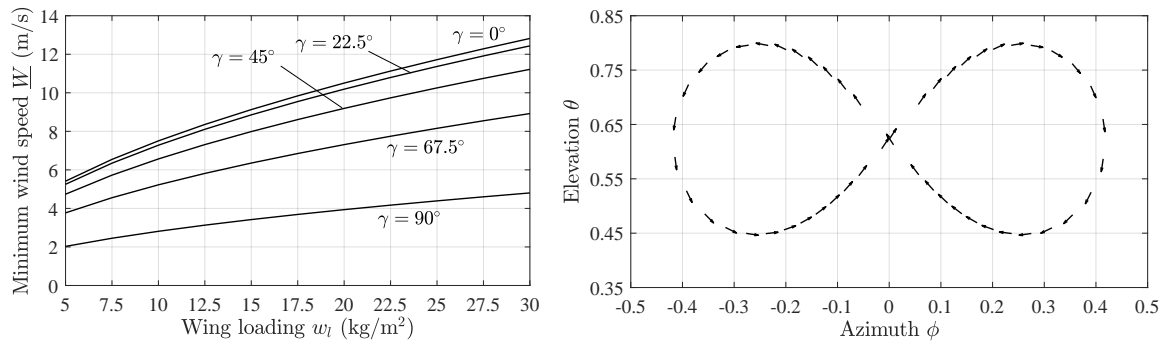


Figure 13

Left: effect of wing loading on the minimum wind speed such that the aircraft can remain airborne without injecting power from ground, with velocity angle γ varying from 0° (flight straight upwards) to 90° (level flight). Parameters: $A = 20 \text{ m}^2$, $C_L = 1.2$, $G = 15$, $d_t = 0.015 \text{ m}$, $l_t = 100 \text{ m}$, $\theta = 35^\circ$, $\phi = 0^\circ$. Right: example of eight-down path in (ϕ, θ) coordinates. The aircraft climbs in the middle and descends when turning at the sides. The vectors are oriented according to the velocity angle γ at each considered point of the path.

It can be noted that the required wind speed grows less than linearly with the wing loading, a result that is intuitive, since for a given lifting surface the aerodynamic forces grow with the square of W , while the weight force grows linearly with w_l . Yet, for straight upwards motion ($\gamma = 0$), \underline{W} might exceed 10 m/s for $w_l \simeq 20 \text{ kg/m}^2$. This value of \underline{W} is close to the typical rated wind speed for a conventional wind generator and much larger than its cut-in wind speed. For $\gamma = 90^\circ$ (level flight), the required wind speed is much lower, about 4 m/s with $w_l = 20 \text{ kg/m}^2$. However, in order to carry out periodic trajectories in crosswind motion, the aircraft must be able to climb with γ of about $45\text{--}60^\circ$, considering figure-eight patterns with so-called “down-loops” or “eight-down”, see e.g. (10) and Figure 13 (right) for an example. According to the presented analysis, with the considered parameters such trajectories could be performed without power injection with W in a rather broad range of $[4, 9] \text{ m/s}$ depending on $w_l \in [5, 20] \text{ kg/m}^2$. The system’s cut-in wind speed would be slightly smaller than \underline{W} , since in principle it is possible to still obtain a positive net power even when part of the crosswind flight must be sustained by injecting energy. The absence of straight-up parts of the trajectory is indeed one of the main advantages of figure-eight patterns with down-loops, as they more likely avoid the need to inject energy from ground to complete the path, differently from circular and “eight-up” trajectories (another advantage being the lower variability of the produced power, see (10)).

The presented analysis can be carried out also for onboard systems, leading to similar results. Overall, it indicates that w_l should be kept as low as possible, as intuition suggests. One can also study its effect on the power conversion performance, showing that it has indeed a significant role. The wing loading is the result of many design choices, such as the type of aircraft (soft or rigid) and its materials, the onboard components, the tether material/technology, the structural resistance, within an overall system design optimization problem that is only partially considered in the literature, see e.g. (65).

4. ACHIEVEMENTS IN AWE AUTOMATION

Control is by far the most actively investigated aspect of AWE systems, because of its relevance as enabling technology and of the complexity of the involved problems. As for all systems that are envisioned to become fully autonomous, AWE generators feature a hierarchical control architecture, visualized in Figure 14. The recent survey (51) provides

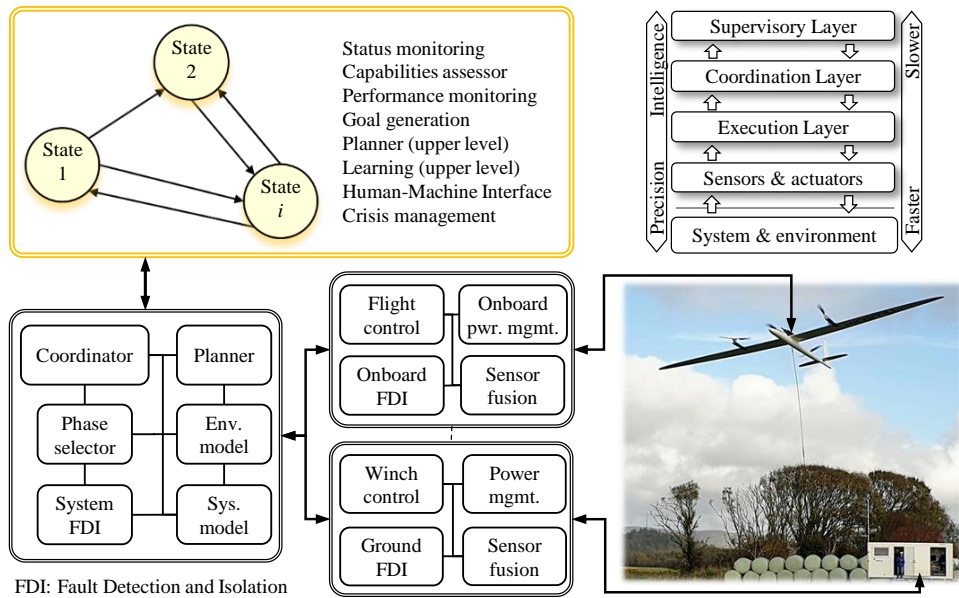


Figure 14

Overview of the hierarchical and distributed automation system of AWE generators. A concept control structure for general autonomous systems is represented in the top-right corner, see e.g. (66, 67), showing the principle of “increasing intelligence and decreasing precision” when climbing the hierarchy.

a complete treatise and list of the literature regarding modeling, estimation, and control aspects of AWE in more than a decade. A critical analysis of the evolution of the literature and of non-published accomplishments by the various companies leads to the following key points: 1) there is a good level of maturity of solutions for all low-level and mid-level control functions, so that today AWE systems can carry out all operational phases automatically under external supervision; 2) there are still significant challenges to reach fully autonomous operation. We substantiate the first point in this section, presenting illustrative results for

each one of the three considered classes, and we specify the standing challenges and related research directions in Section 5.

4.1. Automatic on-ground AWE

Several on-ground AWE developers are testing small-to-medium scale prototypes to accumulate operational hours and the related data, which is required to improve the TPL before up-scaling their systems (see Section 3.1). We present here unpublished results pertaining to the systems of Skysails and Kitemill.

4.1.1. Flexible-wing systems. SkySails Power is constantly carrying out flight tests at its test site in northern Germany with the goal of validating correct functioning and improving all system components, testing new automation features, and gaining experience with different weather conditions. The system installed at the test site is of the same scale as the SKS PN-14 product, see Section 2.1.1. Figure 15 presents the data collected during automatic power generation. Over the first year of operation, several hundred hours of

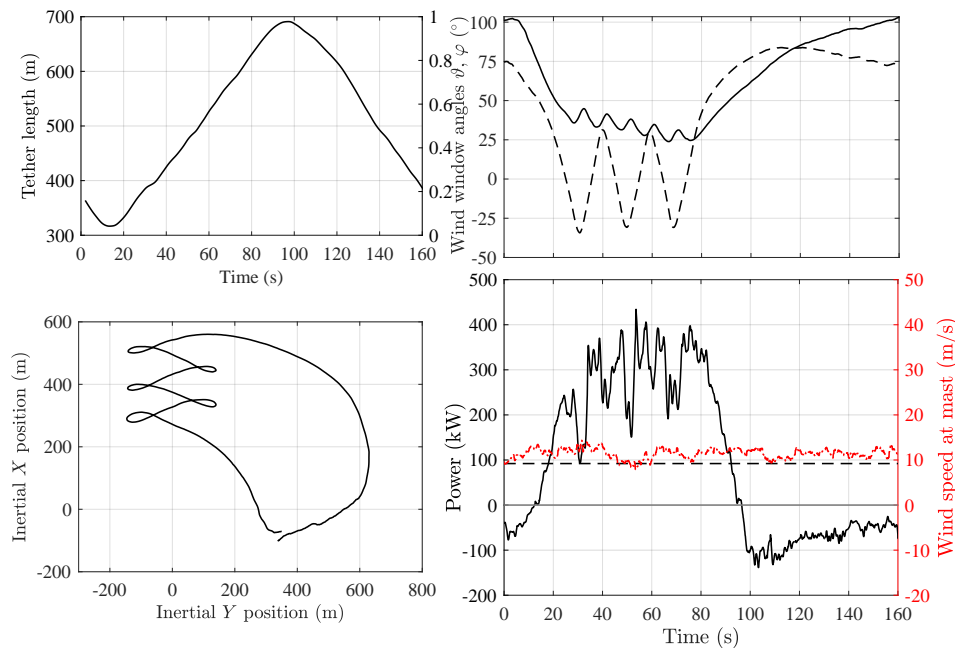


Figure 15

Experimental results. Representative automated power cycle during flight tests at the SkySails Power site in northern Germany in Spring 2021. Clockwise from top-left: tether length (m); wind window angles ($^{\circ}$); mechanical power (solid line, kW), cycle power (dashed, kW) and wind speed at mast height (red dash-dotted line, m/s); X – Y inertial position (m). The average power over the pumping cycle is about 92 kW. For the definition of coordinate system and wind window angles see reference (17).

automated flight have been collected at this test site and the system has encountered wind

speeds ranging between 4 m/s and 23 m/s whilst airborne and in automated power cycle operation. During a specific measuring campaign, an uninterrupted automated flight of 42 hours featuring day and night flight with an average power production of 62 kW has been achieved, in wind conditions varying between 4 m/s and 13 m/s (one minute average measured at 10m height) and estimated wind speeds at flight altitude of 6 m/s to 19m/s, showing the robustness of the implemented flight and power cycle automation algorithms and all system components at relevant load condition. Besides power generation, the company has shown that ram-air kite technology can be used for traction of large marine transport vessels (58) using kite sizes of up to 400 m², proving the scalability of this flexible-wing technology. Moreover, for the application of Yacht propulsion, SkySails has successfully developed and commissioned a system (68, 69) on the marine vessel Race for Water (<https://www.raceforwater.org/en/>). The system has been handed over to the customer and several hundred hours of automated kite flight have helped to propel the yacht, showing the high TPL achieved.

4.1.2. Rigid-wing systems. Kitemill is currently testing extensively with its 20-kW KM1 prototype in supervised automatic operation, gaining know-how and improving on all aspects of the technology. Figure 16 shows recent results with this prototype. While the latest test data of the KM1 and the details of the developed solutions are kept confidential, we report here some of the findings regarding the various operational phases, as well as test data (tether force and speed, kite speed, mechanical power) of the smaller and earlier KM0 prototype, with a wingspan of 4 m, whose aim was to demonstrate system functionality.

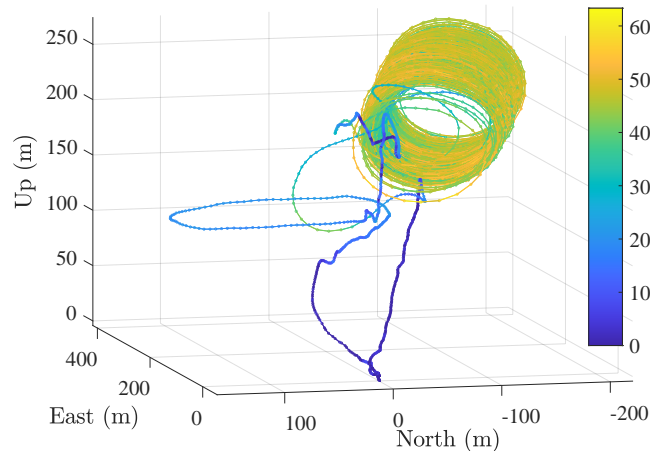


Figure 16

Experimental results with the KM1 prototype. The colorbar indicates the measured airspeed in m/s. The blue lines (low airspeed) denote the phases of the flight in autonomous VTOL. During the take-off, the aircraft moves downwind to where it shall start production. Then, control is switched to manual flight and the winch reels in to do a winch-launch in the air, from where the pilot enters manually into looping. After a few loops, the autopilot is switched on, providing much more consistent trajectories and power production. 45 minutes of autonomous looping are shown. Transition from looping back to hover and vertical landing are shown, too.

About the automatic take-off, thanks to the onboard propellers this phase is rather sim-

ple in normal weather conditions: the kite hovers vertically until a few meters of elevation, then its nose is pitched up so to move diagonally downwind, gaining further altitude by the combined action of aerodynamic lift and propellers, while the tether is reeled-out toward the starting point for looping. The transition from VTOL to crosswind flight is obtained by switching off the propellers and reeling-in the tether while pitching up the aircraft, in a way similar to what done during a winch launch (62) but operated from mid-air. In the traction phase, loops are being carried out instead of figure-eights. Autonomous looping is obtained by following a circular trajectory that lies on a plane angled with a chosen average elevation and azimuth angles. As the tether is reeled-out, the plane is accordingly shifted outwards from the ground station, and the kite moves on the surface of a cylinder. The tracking problem is solved by linear controllers, with an approach similar to, e.g., (22). Regarding landing, the aircraft is switched back to VTOL mode with position feedback, then it moves to a position close to the landing platform and it is switched to attitude control. Finally, the winch gradually brings the aircraft to a landing on the VTOL platform while the kite maintains a roughly constant attitude. During the tests, the mentioned approaches proved to be repeatable in all the encountered wind conditions, and also robust to unexpected events like strong wind gusts which led to rather large perturbations, such as a complete 360° yaw maneuver during take-off, accompanied by large pitch and roll motion. Regarding performance during automatic pumping cycles, Figures 17-18 present typical courses of the involved variables.

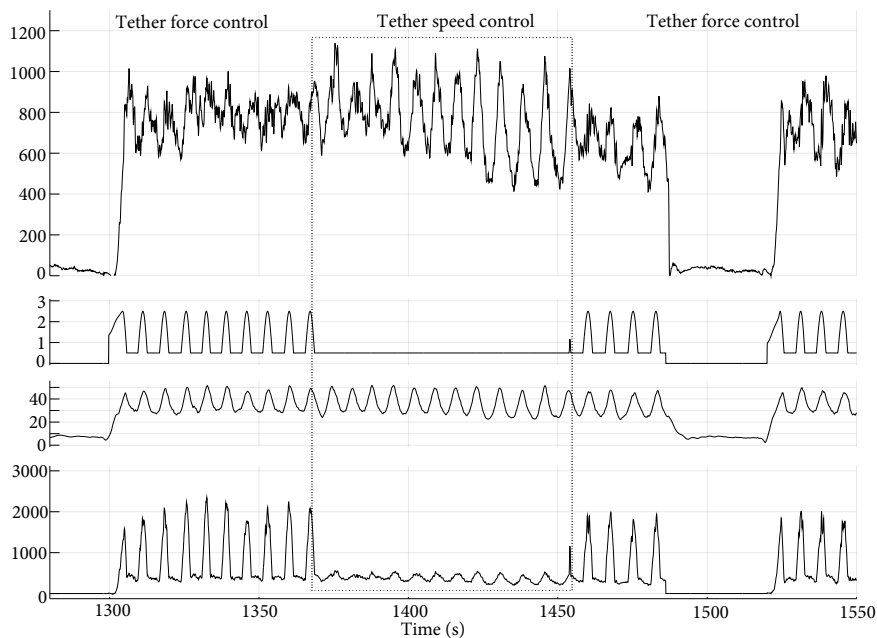


Figure 17

Experimental results with Kitemill's KM0 functional prototype. From top to bottom: tether force (N), reel-out speed (m/s), kite speed (m/s), produced power (W). In the dotted frame, a constant reel-out velocity is commanded, while outside the frame a force control system is engaged. It can be noted that at constant reel-out speed the power performance is worse.

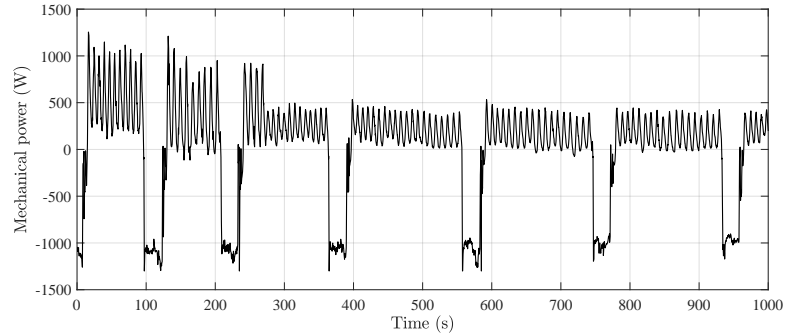


Figure 18

Experimental results with Kitemill’s KM0 functional prototype. Generated mechanical power over several pumping cycles.

4.2. Automatic onboard AWE

The reports (55) contain extensive information on the control system and flight controller of the Makani M600 prototype, as well as a critical analysis of its weaknesses. We refer the reader to these documents for the details. Here, we present experimental results on kiteKRAFT’s small-scale functional prototype, and their comparison with simulations developed by the company. Indeed, while for on-ground systems a large number of contributions exist regarding modeling and simulation (51), there is currently much less material for onboard ones, with the exception of said reports (55) and few other contributions focused on the power electronics, like (70, 71). An important part of the development work at kiteKRAFT is focused on the engineering model (“digital twin”) to predict the behavior of the real system and to enable a successful functioning of the control software. The modeling and controller development are based on first-order principles as much as possible. As a specific example, the employed aerodynamics model in kiteKRAFT’s control design and real-time simulation is the coupled/nonlinear vortex lattice wing (blade) element momentum (VLWEM) theory, similar to (72) (section 6.2), extended with rotor-wing interactions. Each wing is span-wise subdivided in finite elements, each one with a vortex horseshoe and 2D airfoil polars based on CFDs or wind tunnel data. The vortex strength of each wing element is calculated by solving the coupled aerodynamics equations such that the lift calculated with the Kutta-Joukowski theorem is equal to the lift calculated with the 2D airfoil polars (which depends on the effective angle of attack and thus on all vortices). The in-house developed solution algorithm can be executed faster than real-time, is guaranteed to never diverge, and usually finds the solution with a few iteration steps only. This enables finding in real-time (in the ms range) the flaperon positions in the control allocation to meet the desired moments demanded by the PID attitude controllers. The VLWEM-model is valid also in non-linear regions including actuator saturations, post-stall, and hovering, where the angle of attack is approximately 90° . Moreover, it covers the various rotor states and thereof induced velocities, specifically also during propeller mode and wind turbine mode, solving the problems described by Makani engineers in (73). This approach also reduces the need for flight testing campaigns purely aimed at model identification and controller tuning. Possible failures of some control surfaces are naturally handled by the control allocation as well. Once the VLWEM-model and the related controllers are validated, a scaled-up or

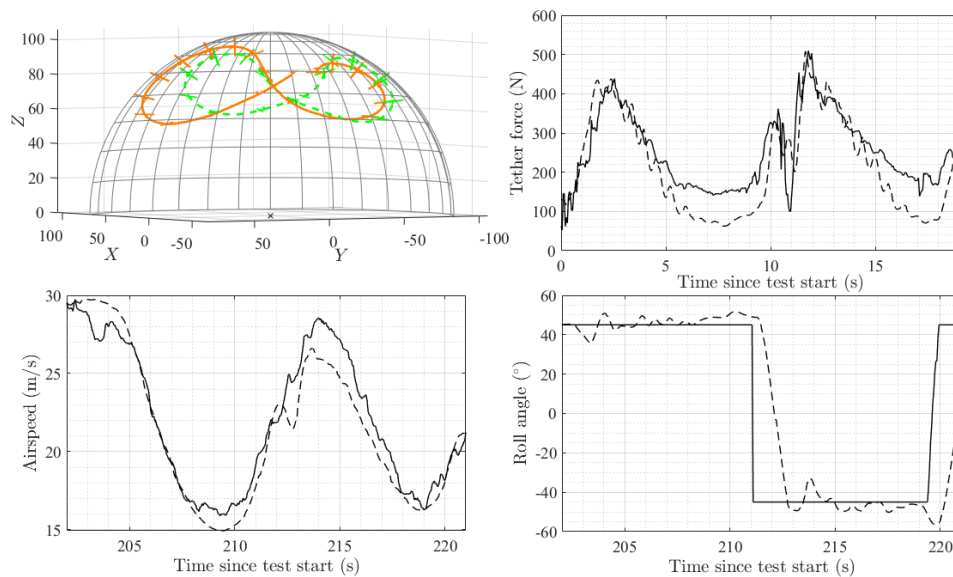


Figure 19

Experimental results with kiteKRAFT functional prototype. Clockwise from top-left: 1) Measurement (orange) and simulation (green) of position and attitude in one second intervals during a figure eight flight. The asymmetric matching between left and right sides is due to an uneven trim of the elevator during the tests; 2) Measured tether force (dashed) and its real-time prediction by the VLWEM-model (solid), indicating a good matching; 3) Airflow speed measured by a pitot tube (solid) and via GNSS and Kalman filtering (dashed); 4) Roll angle control performance: actual roll (dashed) and reference (solid). The roll angle controller is linear, the nonlinear nature of the aerodynamics being covered by the control allocation, which solves the VLWEM-model and finds the right flaperon positions to actuate the demanded roll moment.

otherwise improved aircraft (e.g., improved airfoil or wing configuration) is likely to work right away. Examples of the model accuracy against experimental data are described next, in various conditions.

One of the first tests to validate the described VLWEM approach was to hover the kite and disturb it in hover-yaw direction (i.e., roll-direction in airplane/kite coordinates (73, 55), see Figure 9). Since the yaw moment that the rotors can exert by differential speeds is negligibly small (relative to the large inertia of the wings), another means of yaw control authority is required, which is solved by mounting the rotors in front of the boxplane wings close to the wing tips, and use the flaperons for thrust vectoring or lift augmentation, respectively. The lack of hover-yaw control authority of Makani's configuration caused in fact several crashes and almost-crashes, see (59) for more details. Reference (74) shows a video of a stress test of the hover-yaw control with the VLWEM approach. As visible, the kite is stabilized rather quickly and with little overshoot, as expected from simulation runs. Several hovering tests with various tether lengths and test conditions have been conducted, including high hover at up to about 20 m from ground and with strong side-ward wind up to about 10 m/s plus gusts. In all cases, the controller rejected disturbances and kept the kite's attitude at the demanded angles within a close error band of a few degrees. Finally, regarding automatic crosswind flight, Figure 19 presents experimental data related to the test session visible at (75),(76).

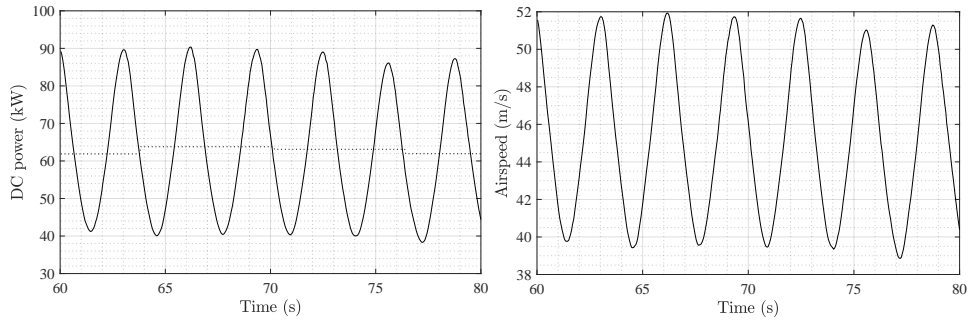


Figure 20

Simulation results of kiteKRAFT 100-kW system under development, considering 10 m/s wind speed at 100 m altitude. A figure-eight lasts about 6 s, and has an extension of about 20° vertically and $\pm 30^\circ$ horizontally. The power is slightly above 60 kW on average and oscillates between about 40 kW and 90 kW. The airspeed is between 40 and 52 m/s. At 12 m/s wind speed and 100 m altitude, the currently design-intended 100kW average power is reached (not shown here).

The tests conducted so far indicate that the developed model can predict rather accurately the real system behavior, as also partly shown in Figure 19, thus increasing the confidence in using it to estimate the behavior of larger systems. To this regard, Figure 20 presents simulation results for the planned 100 kW product, based on the current status of development and assumptions imposed in the simulation model. To reduce the power oscillations during a path, in particular at large scale in wind farm operation, currently the best envisioned approach is to phase-shift the positions of two or more systems. This will have likely only the effect of added software-complexity, and a negligible efficiency reduction.

5. AUTONOMOUS AWE: CHALLENGES AHEAD

As experimental testing of automatic, supervised AWE operation is increasingly picking up pace, the resulting knowledge allows developers to optimize the plant and reach higher levels of reliability, in a virtuous circle that will further accelerate the development progress. The presence of market segments where AWE systems in the range of 100-KW average power are attractive, as demonstrated by the commercialization of the SKS PN-14, is a crucially important element that strengthens the feeling that the path to large-scale AWE industrialization is feasible with continued support and R&D efforts. To be a valid technology for large scale wind power conversion, AWE systems will need to: a) be larger (in the range of a few MW per unit), b) operate in large-scale farms, and c) be fully autonomous, requiring minimal supervision. The challenges to be met to realize these three goals encompass many disciplines (5); we point out here those related to automation and control. We believe that automatic operation in nominal and healthy conditions won't be a fundamentally difficult challenge at large scale, in light of the described accomplished results and ongoing activities. On the other hand, we believe that the most important problems to be solved, requiring also fundamental research and new analysis/design methods, pertain to 1) all-round automation also in out-of-nominal conditions, and 2) system robustness and fault tolerance. We provide next specific instances pertaining to each one of these two areas.

- **Out-of-nominal and time-varying conditions.** For AWE systems, wind is the resource to be harvested, but also the “fuel” that keeps the aircraft airborne, and

partly a disturbance to be rejected. We are not aware of other complex autonomous systems that feature the same relationships with exogenous signals. The wind velocity is a time-varying 3D vector field, typically only measurable at a few points in space. Its effects on the aircraft are also relatively unpredictable, due to the complex physics of flows: the Navier-Stokes equations, which describe these phenomena, are strongly and stiffly coupled partial differential equations. Airfoil performance may be also highly subject to surface roughness or manufacturing accuracies, even for standard literature airfoils, and several AWE developers are designing and building airfoil configurations that are new with respect to the state of the art.

AWE automation systems will need to master the various wind conditions, their change over time, which can be very fast, and their effects on the system. This requires constantly inferring and predicting the wind conditions, and consequently making sensible choices in terms of flown trajectories (since choosing to fly in an area with too little wind or incompatible wind/tether directions might lead to controllability problems). On-ground systems will also have to always evaluate whether each candidate decision is too risky given the available stored energy. Possible candidate methods to deal with this problem shall be able to use operational data to learn about site-specific features and patterns, in order to gradually improve performance over time, while being able to enforce safety for a wide range of conditions, also rare and sudden ones, such as extreme weather and sudden gust from any side during the relatively short transition phases. Even simulating such rare events is per-se a challenge, considered by few contribution only (44).

- **Plant-wide automation and safety-responsibility.** Even when there is no fault in any of its components, an AWE system may cause damage to itself or to the environment, due to the uncertain nature of wind. Thus, the supervisory control logic shall be able to actively guarantee low operational risk, always trading off safety and performance. It shall understand when the available information is good enough to take a safe decision, e.g. whether to take-off or to move the flown trajectories to a different region of the airspace. We term this feature safety-responsibility. It is an open challenge to design safety-responsible automation systems that are provably so, under some realistic assumptions. At higher wind speed the system will need to operate close to its constraints. Whereas large safety margins are acceptable at first, there is a push to reduce these margins as much as possible to increase the profitability of the system yet without reducing its reliability. This is linked to topics such as design and verification of complex, nonlinear hybrid systems, where there are still many open problems. Validating an AWE system in practice is clearly prohibitive, simply because the number of specific operating scenarios it may encounter is infinite, and the most critical ones usually tend to be very rare, as argued above. Safety-responsible control also requires coverage of the full flight envelope to avoid conditions where no action is taken, because it falls outside the a-priori foreseen ones. Realizing that the current condition falls outside the manifold of planned behaviors may be itself a challenge, connected to fault detection. Perfect coordination among the various hierarchical levels and in the transitions between all operation phases is also required. For example, winch-tether-kite interactions and their effects on flight mechanics need to be better understood, as they also play an important role in high-level decisions.
- **Multi-agent management.** When more than one AWE systems will be installed in wind farms, the problem of how their operation shall be synchronized will be

critical. The interactions among several systems are currently investigated only via simulations. Such a coordination may be beneficial for many aspects, such as easier grid integration and more effective power extraction (by limiting the wake effects). Coordination of multiple AWE systems in a park to minimize storage requirements and space utilization is a topic of ongoing research (77). This problem is difficult (and open) due to the same uncertainty sources that also affect a single AWE system, plus the additional complexity arising with multiple units.

- **Simplicity.** A main challenge is to keep control of the complexity of the entire system. AWE systems have in common, that they are extracting energy from an a-priori unknown wind field by using a 3D flight trajectory. This is already a quite complex task, due to the existing system and dynamics constraints. An important design philosophy is to avoid adding unnecessary complexity to the system, as this brings the risk of higher maintenance cost, more difficult failure cause investigations and increased documentation costs. This also applies to control and automation solutions, which shall then be the simplest ones that accomplish the desired functionality. Control solutions can also help to simplify the system, and vice-versa. A concrete example are the figure-of-eight paths for onboard systems like kiteKRAFT's kites, which not only enables flying with few control actuators at high winds (see (78)), but also does not require a slip ring at the ground station to allow the tether to rotate indefinitely. Another example is a proper mechanical design of the actuators, to reduce the control effort.
- **Fault tolerance.** However, there are essential parts and essential complexities that can not be avoided. For example, for robustness and redundancy, several sensors must be mounted on the kite and ground station at least twice, and redundancy of the control units shall be considered as well. The software must be endowed with suitable fault detection, isolation, and recovery algorithms at all levels. This is because AWE generators are safety-critical systems, so that components' failures can lead to substantial damage. High safety and reliability thus requires a high level of fault tolerance; control design and analysis methods shall be combined with safety-oriented system engineering to guarantee that critical events happen with close-to-negligible risk, for example by guaranteeing operation (possibly degraded) under any single point of failure. While usually these aspects are technology-specific, so that it is difficult to derive and exploit general methods, a more fundamental challenge pertains to how the autonomous system shall take into consideration possible faults when planning its next moves.

6. CONCLUSIONS

The Airborne Wind Energy sector is thriving with research and development activities and reaching even higher goals at increasing speed. Strong attention of the public opinion and policy makers on sustainability and environment preservation and future scenarios where the power demand might double in the next 20 years, due to transport electrification, provide a fertile ground to foster AWE development and industrialization. Indeed, companies have rather ambitious scaling objectives, yet today more than ever realistic assuming enough funding and public support. For example, SkySails envisions a next scaling step with kite sizes in the range 500-700 m², which in combination with a scaled-up ground station, aerodynamic improvements and power cycle improvements are expected to achieve average

cycle power at MW-scale at adequate sites. Similarly, Kitemill has planned for a 350-500-kW system in 2025, and MW-scale ones in 2029, while kiteKRAFT considers a first 100-kW series product in 2024 with subsequent scaling steps at 0.5MW up to 3MW for a single unit, with an R&D trajectory that favors TPL before TRL (79). We believe that scientific communities can play a crucial role to facilitate this process, at the same time addressing fundamentally difficult and theoretically challenging problems, some of which have been described in this review paper. The entry level for research in AWE may be perceived as high, especially regarding real-world testing at medium and large scale. For this reason, private-public collaboration models such as joint research centers, partnerships, and actions facilitated by public funding (like the EU Framework Programmes for Research and Innovation) shall be deployed to best exploit the complementary skills of industrial and academic players.

DISCLOSURE STATEMENT

The authors are not aware of any affiliations, other than those stated in the title page, memberships, funding, or financial holdings that might be perceived as affecting the objectivity of this review.

ACKNOWLEDGMENTS

The authors thankfully acknowledge the great work by the SkySails team, the kiteKRAFT team, and the Kitemill team - all who in one way or another helped shape the results presented in this paper.

LITERATURE CITED

1. Bauer F. 2019. Do We Need Flying Wind Turbines? (Spoiler: Absolutely!), <https://medium.com/kitekraft/do-we-need-flying-wind-turbines-spoiler-absolutely-858da214306e>
2. Manalis MS. 1976. Airborne windmills and communication aerostats. *Journal of Aircraft* 13(7):543–544
3. Loyd ML. 1980. Crosswind kite power. *Journal of Energy* 4(3):106–111
4. International Renewable Energy Agency (IRENA), Abu Dhabi. 2016. Innovation Outlook: Off-shore Wind.
5. European Commission - Directorate-General for Research and Innovation. 2018. Study on Challenges in the commercialisation of airborne wind energy systems. [Online] Last accessed 21 May 2021
6. Ilzhöfer A, Houska B, Diehl M. 2007. Nonlinear MPC of kites under varying wind conditions for a new class of large-scale wind power generators. *International Journal of Robust and Nonlinear Control* 17:1590–1599
7. Canale M, Fagiano L, Milanese M. 2010. High altitude wind energy generation using controlled power kites. *IEEE Transactions on Control Systems Technology* 18(2):279–293
8. Fagiano L, Milanese M, Piga D. 2011. Optimization of airborne wind energy generators. *International Journal of Robust and Nonlinear Control* 22(18):2055–2083
9. Fagiano L, Zraggen A, Morari M, Khammash M. 2014. Automatic crosswind flight of tethered wings for airborne wind energy: modeling, control design and experimental results. *IEEE Transactions on Control Systems Technology* 22(4):1433–1447
10. Erhard M, Strauch H. 2015. Flight control of tethered kites in autonomous pumping cycles for airborne wind energy. *Control Engineering Practice* 40:13–26

11. Erhard M, Horn G, Diehl M. 2017. A quaternion-based model for optimal control of an airborne wind energy system. *ZAMM - Journal of Applied Mathematics and Mechanics / Zeitschrift für Angewandte Mathematik und Mechanik* 97(1):7–24
12. Gupta Y, Dumon J, Hably A. 2017. Modeling and control of a magnus effect-based airborne wind energy system in crosswind maneuvers. *IFAC-PapersOnLine* 50(1):13878–13885, 20th IFAC World Congress
13. Li H, Olinger D, Demetriou M. 2018. Attitude tracking control of an airborne wind energy system. *Green Energy and Technology*. Springer, 215–239
14. Baheri A, Bin-Karim S, Bafandeh A, Vermillion C. 2017. Real-time control using Bayesian optimization: A case study in airborne wind energy systems. *Control Engineering Practice* 69:131–140
15. Ahbe E, Wood TA, Smith RS. 2018. *Transverse Contraction-Based Stability Analysis for Periodic Trajectories of Controlled Power Kites with Model Uncertainty*. In *2018 IEEE Conference on Decision and Control (CDC)*, pp. 6501–6506. Miami Beach, FL, USA
16. Wood TA, Hesse H, Polzin M, Ahbe E, Smith RS. 2018. Modeling, identification, estimation and adaptation for the control of power-generating kites. *IFAC-PapersOnLine* 51(15):981–989 18th IFAC Symposium on System Identification SYSID 2018
17. Erhard M, Strauch H. 2018. Automatic control of pumping cycles for the skysails prototype in airborne wind energy. Singapore: Springer Singapore, 189–213
18. Rapp S, Schmehl R, Oland E, Haas T. 2019. Cascaded pumping cycle control for rigid wing airborne wind energy systems. *J. of Guidance, Control, and Dynamics* 42(11):2456–2473
19. Stastny T, Ahbe E, Dangel M, Siegwart R. 2019. *Locally Power-Optimal Nonlinear Model Predictive Control for Fixed-Wing Airborne Wind Energy*. In *Proceedings of the 2019 American Control Conference (ACC)*, pp. 2191–2196. Philadelphia, PA, USA
20. Cobb MK, Barton K, Fathy H, Vermillion C. 2020. Iterative learning-based path optimization for repetitive path planning, with application to 3-D crosswind flight of airborne wind energy systems. *IEEE Transactions on Control Systems Technology* 28(4):1447–1459
21. Dief TN, Fechner U, Schmehl R, Yoshida S, Rushdi MA. 2020. Adaptive flight path control of airborne wind energy systems. *Energies* 13(3):667
22. Todeschini D, Fagiano L, Micheli C, Cattano A. 2021. Control of a rigid wing pumping airborne wind energy system in all operational phases. *Control Engineering Practice* 111:104794
23. Fechner U, van der Vlugt R, Schreuder E, Schmehl R. 2015. Dynamic model of a pumping kite power system. *Renewable Energy* 83:705–716
24. Licitra G, Bürger A, Williams P, Ruiterkamp R, Diehl M. 2018. Optimal input design for autonomous aircraft. *Control Engineering Practice* 77:15–27
25. Pastor-Rodriguez A, Sanchez-Arriaga G, Sanjurjo-Rivo M. 2017. Modeling and Stability Analysis of Tethered Kites at High Altitudes. *Journal of Guidance Control and Dynamics* 40(8):1892–1901
26. Sanchez-Arriaga G, Garcia-Villalba M, Schmehl R. 2017. Modeling and dynamics of a two-line kite. *Applied Mathematical Modelling* 47:473–486
27. Fagiano L, Huynh K, Bamieh B, Khammash M. 2014. On sensor fusion for airborne wind energy systems. *IEEE Transactions on Control Systems Technology* 22(3):930–943
28. Schmidt E, De Lellis Costa de Oliveira M, Saraiva da Silva R, Fagiano L, Trofino Neto A. 2020. In-flight estimation of the aerodynamics of tethered wings for airborne wind energy. *IEEE Transactions on Control Systems Technology* 28(4):1309–1322
29. Paulig X, Bungart M, Specht B. 2013. Conceptual design of textile kites considering overall system performance. In *Airborne Wind Energy*, ed. U Ahrens, M Diehl, R Schmehl, pp. 547–562. Berlin Heidelberg: Springer
30. Bosman R, Reid V, Vlasblom M, Smeets P. 2013. Airborne wind energy tethers with high-modulus polyethylene fibers. Berlin, Heidelberg: Springer Berlin Heidelberg, 563–585
31. Vimalakanthan K, Caboni M, Schepers J, Pechenik E, Williams P. 2018. Aerodynamic analysis

- of Ampyx’s airborne wind energy system. *J. of Physics: Conf. Series* 1037:062008
32. De Lellis M, Reginatto R, Saraiva R, Trofino A. 2018. The Betz limit applied to Airborne Wind Energy. *Renewable Energy* 127:32–40
 33. Vander Lind D. 2013. Analysis and flight test validation of high performance airborne wind turbines. In *Airborne Wind Energy*. Berlin Heidelberg: Springer
 34. Bauer F, Kennel RM, Hackl CM, Campagnolo F, Patt M, Schmehl R. 2018. Drag power kite with very high lift coefficient. *Renewable Energy* 118:290–305
 35. Licitra G, Koenemann J, Bürger A, Williams P, Ruiterkamp R, Diehl M. 2019. Performance assessment of a rigid wing Airborne Wind Energy pumping system. *Energy* 173(C):569–585
 36. Ruiterkamp R, Sieberling S. 2014. Airborne wind energy, chap. 26. “Description and Preliminary Test Results of a Six Degrees of Freedom Rigid Wing Pumping System”. Green Energy and Technology. Berlin: Springer-Verlag, 443–458
 37. Luchsinger R, Aregger D, Bezaud F, Costa D, Galliot C, et al. 2018. Airborne wind energy, advances in technology development and research, chap. 24. “Pumping Cycle Kite Power with Twings”. Green Energy and Technology. Berlin: Springer-Verlag, 603–621
 38. Stuyts J, Horn G, Vandermeulen W, Driesen J, Diehl M. 2015. Effect of the electrical energy conversion on optimal cycles for pumping airborne wind energy. *IEEE Transactions on Sustainable Energy* 6(1):2–10
 39. Fagiano L, Milanese M, Piga D. 2010. High-altitude wind power generation. *IEEE Transactions on Energy Conversion* 25(1):168–180
 40. Heilmann J, Houle C. 2013. Economics of pumping kite generators. In *Airborne Wind Energy*, ed. U Ahrens, M Diehl, R Schmehl, pp. 271–284. Berlin Heidelberg: Springer
 41. Malz E, Hedenus F, Göransson L, Verendel V, Gros S. 2019. Drag-mode airborne wind energy vs. wind turbines: An analysis of power production, variability and geography. *Energy* :116765
 42. Haas T, Schutter JD, Diehl M, Meyers J. 2019. *Wake characteristics of pumping mode airborne wind energy systems*. In *Journal of Physics: Conference Series, Wake Conference 2019*, vol. 1256. Visby, Sweden
 43. Salma V, Friedl F, Schmehl R. 2019. Improving reliability and safety of airborne wind energy systems. *Wind Energy* 23(2):340–356
 44. Rapp S, Schmehl R. 2021. Enhancing resilience of airborne wind energy systems through upset condition avoidance. *Journal of Guidance, Control, and Dynamics* 44(2):251–265
 45. Archer CL, Caldeira K. 2009. Global assessment of high-altitude wind power. *Energies* 2(2):307–319
 46. Archer CL, Delle Monache L, Rife DL. 2014. Airborne wind energy: Optimal locations and variability. *Renewable Energy* 64:180–186
 47. Bechtle P, Schelbergen M, Schmehl R, Zillmann U, Watson S. 2019. Airborne wind energy resource analysis. *Renewable Energy* 141:1103–1116
 48. Fagiano L, Milanese M. 2012. *Airborne Wind Energy : an overview*. In *Proceedings of the 2012 American Control Conference*, pp. 3132–3143. Montréal, Canada: IEEE
 49. Cherubini A, Papini A, Vertechy R, Fontana M. 2015. Airborne wind energy systems: A review of the technologies. *Renewable and Sustainable Energy Reviews* 51:1461–1476
 50. Mendonça de Souza AKdS, Vaz Rodrigues C, Lezana AGR, Anacleto CA, Paladini EP. 2017. Comparing patent and scientific literature in airborne wind energy. *Sustainability* 9(6)
 51. Vermillion C, Cobb M, Fagiano L, Leuthold R, Diehl M, et al. 2021. Electricity in the air: Insights from two decades of advanced control research and experimental flight testing of airborne wind energy systems. *Annual Reviews in Control*
 52. Ahrens U, Diehl M, Schmehl R, ed. 2013. *Airborne Wind Energy*. Berlin Heidelberg: Springer
 53. Schmehl R, ed. 2018. *Airborne Wind Energy - Advances in Technology Development and Research*. Singapore: Springer
 54. Makani Power. 2021. Pulling power from the sky: The story of makani [feature film]
 55. Makani Power. 2021. The Energy Kite Parts I, II, and III

56. SkySails GmbH. 2021. Series production of AWES starts, <https://skysails-power.com/series-production-of-awes-starts/>
57. Erhard M, Strauch H. 2013. *Sensors and navigation algorithms for flight control of tethered kites*. In *2013 European Control Conference (ECC)*, pp. 998–1003
58. Erhard M, Strauch H. 2012. Control of towing kites for seagoing vessels. *IEEE Transactions on Control Systems Technology* 21(5):1629–1640
59. Bauer F. 2020. Taking over the Baton from Makani, <https://medium.com/kitekraft/taking-over-the-baton-from-makani-23318d88b7b0>
60. Bauer F, Kennel RM. 2018. Fault tolerant power electronic system for drag power kites. *Journal of Renewable Energy (Hindawi)*
61. Schmehl R, Noom M, van der Vlugt R. 2013. Traction power generation with tethered wings. In *Airborne Wind Energy*, ed. U Ahrens, M Diehl, R Schmehl, pp. 23–45. Berlin Heidelberg: Springer
62. Fagiano L, Schnez S. 2017. On the take-off of airborne wind energy systems based on rigid wings. *Renewable Energy* 107:473–488
63. Houska B, Diehl M. 2007. *Optimal control for power generating kites*. In *Proceedings of the 9th European Control Conference*, pp. 3560–3567. Kos, Greece
64. Trevisi F, Gaunaa M, McWilliam M. 2020. The influence of tether sag on airborne wind energy generation. *Journal of Physics: Conference Series* 1618:032006
65. Trevisi F, McWilliam M, Gaunaa M. 2021. Configuration optimization and global sensitivity analysis of ground-gen and fly-gen airborne wind energy systems. *Renewable Energy*, DOI: <https://doi.org/10.1016/j.renene.2021.06.011>
66. Antsaklis PJ, Passino KM, Wang SJ. 1991. An introduction to autonomous control systems. *IEEE Control Systems Magazine* 11(4):5–13
67. Passino KM. 1995. Intelligent control for autonomous systems. *IEEE Spectrum* 32(6):55–62
68. Quack M. 2017. Recent advances in automation of tethered flight at skysails power. *Oral presentation at AWEC 2017, Freiburg, Germany, 2017*, <https://awec2017.com/presentations/manfred-quack>
69. Quack M. 2017. Extended periods of automated tethered flight at skysails. *Oral presentation at AWEC 2019, Glasgow, Scotland, 2019*, <https://av.tib.eu/media/50214>
70. Kolar JW, Friedli T, Krismer F, Looser A, Schweizer M, et al. 2013. Conceptualization and multiobjective optimization of the electric system of an airborne wind turbine. *IEEE Journal of Emerging and Selected Topics in Power Electronics* 1(2):73–103
71. Gammeter C, Krismer F, Kolar JW. 2016. Comprehensive conceptualization, design, and experimental verification of a weight-optimized all-sic 2 kv/700 v dab for an airborne wind turbine. *IEEE Journal of Emerging and Selected Topics in Power Electronics* 4(2):638–656
72. van Dam C. 2002. The aerodynamic design of multi-element high-lift systems for transport airplanes. *Progress in Aerospace Sciences* 38(2):101–144
73. Makani Power documentation. 2020. https://github.com/google/makani/blob/1d66923243f73a69cddda52082fd5415907afc99/documentation/control/aero/aero_spec.tex
74. kiteKRAFT. 2020. Hover-yaw control tests, <https://youtu.be/xNPgqNaoMR8>
75. kiteKRAFT. 2020. kiteKRAFT Operational Flight, <https://youtu.be/sc4RAtpwNRw>
76. kiteKRAFT. 2020. kiteKRAFT - Building Flying Wind Turbines, <https://youtu.be/F9gq9Bp3-Jg>
77. Bagaber B, Mertens A. 2021. Fault ride-through performance of pumping cycle airborne wind energy generators with the support of optimally sized energy storage system. *12th International Conference on Electrical and Electromechanical Energy Conversion (ECCE Asia 2021)*
78. Bauer F, Petzold D, Kennel RM, Campagnolo F, Schmehl R. 2018. Control of a drag power kite over the entire wind speed range. *Journal of Guidance, Control, and Dynamics*
79. Weber J. 2012. WEC Technology Readiness and Performance Matrix – finding the best research technology development trajectory. *Available on ResearchGate*